RSC Advances

PAPER

View Article Online
View Journal | View Issue

Cite this: *RSC Adv.*, 2023, **13**, 31925

Super tough and high adhesive eutectic ionogels enabled by high-density hydrogen bond network†

Li Jin,[a] Su Ju,[a] Yiming Zhao,[a] Suli Xing,[a] Jun Tang,[a] Yonglyu He,[a] Chen Chen,[a] Gengyuan Liang*[b] and Jianwei Zhang*[a]

Ionogels have attracted tremendous interest for flexible electronics due to their excellent deformability, conductivity, and environmental stability. However, most ionogels suffer from low strength and poor toughness, which limit their practical applications. This article presents a strategy for fabricating ionogels with high toughness by constructing high-density hydrogen bonds within their microstructure. The ionogels exhibit a maximum fracture strength of 11.44 MPa, and can sustain a fracture strain of 506%. They also demonstrate a fracture energy of 27.29 MJ m^{-3} and offer a wide range of mechanical property adjustments (fracture stress from 0.3 to 11.44 MPa, fracture strain from 506% to 1050%). Strain sensors assembled with ionogels demonstrate exceptional sensing performance and enable motion detection of human joints. This study provides a new approach for achieving strong and tough ionogel design used for high-performance flexible electronic applications.

Received 29th July 2023
Accepted 18th October 2023

DOI: 10.1039/d3ra05120j

rsc.li/rsc-advances

Introduction

In recent years, ionogels have attracted significant attention due to their outstanding stretchability, high ionic conductivity,[1–6] and excellent chemical stability.[7,8] They have shown great potential in various fields such as electronic skin,[9] wearable electronic devices,[10] soft robotics,[11] and biomedicine,[12] where they can convert their deformation information into electrical signals such as resistance, capacitance, and current. Despite substantial effort has been devoted to the development of high-performance ionogels, most of them exhibit low fracture strength (<1 MPa) and poor toughness (<1 MJ m^{-3}),[13–15] which greatly limits their application range and lifespan.

Currently, the common strategies for enhancing the toughness of ionogel materials primarily involve microstructure design and molecular bonding design. The former includes the design of microphase separation structures and the incorporation of nano-reinforcements.[16,17] Through constructing specific microstructures, the fracture strength and fracture toughness of ionogels can be effectively improved. However, this approach involves complex fabrication processes and high costs, which are not practical for large-scale applications. The latter approach mainly involves the introduction of dynamic covalent bonds or non-covalent dynamic interactions as sacrificial networks for achieving toughening in ionogels.[18] The introduction of dynamic covalent bonds in the ionogels has relatively low density, resulting in limited improvement in the toughness of the ionogel.[19] Non-covalent dynamic interactions mainly include ionic bonds and hydrogen bonds. It is common to introduce metal cations (such as Fe^{3+} and Al^{3+}) and carboxylic compounds in ionogels to form ionic coordination bonds.[25] However, ionic bonds raise higher requirements on the polymer functional groups, and the introduction of high concentrations of metal salt ions may cause ionogel aggregation or discoloration.[20] Hydrogen bonding, as a type of intermolecular interaction, is widely present between solvents and polymer molecules. It can be utilized in ionogels to introduce a high density of hydrogen bonds between the solvent and polymers, effectively enhancing the fracture strength of the ionogels.[21] Moreover, hydrogen bonding does not impede the movement of polymer segments, allowing the ionogels to maintain good deformability. Therefore, constructing a high-density hydrogen bond network holds the potential to further enhance the mechanical properties of ionogels.

The density of hydrogen bonds in ionogels is determined by the solvent and polymer matrix. Deep eutectic solvents (DES) are binary or ternary mixtures composed of hydrogen bond donors (polyols, urea, and carboxylic acids, *etc.*) and hydrogen bond acceptors (such as quaternary ammonium salts, choline chloride) in specific molar ratios.[22,23] Within DES, a large amount of hydrogen bond donors and acceptors are present, along with inorganic salt ions that facilitate faster transport. This combination effectively enhances the mechanical performance and ionic conductivity of ionogels. Furthermore, DES offers several advantages over traditional ionic liquids, including lower cost, ease of preparation and storage, and

[a]*College of Aerospace Science and Engineering, National University of Defense Technology, Changsha 410073, China. E-mail: jianwei_zhang@nudt.edu.cn*
[b]*High Speed Aerodynamics Institute, China Aerodynamics Research and Development Center, Mianyang 621000, China. E-mail: lgy940612@163.com*

† Electronic supplementary information (ESI) available. See DOI: https://doi.org/10.1039/d3ra05120j

environmental friendliness, making it an ideal alternative for ionic liquids.[24] Zhang *et al.* utilized a polymerizable deep eutectic solvent (PDES) to prepare highly tough and conductive elastomers with a fracture stress of 5 MPa, fracture strain of 900%.[25] Wang *et al.* achieved excellent mechanical properties (*e.g.*, fracture strain of 2300% and fracture stress of 0.21 MPa) and high conductivity (0.22 mS cm^{-1}) in ionogels by reducing the density of hydrogen bonds within the ionogel.[26] Their work demonstrates that utilizing eutectic solvents can prepare ionogels with excellent mechanical properties, and optimization of the ionogel's mechanical performance can be achieved by adjusting the hydrogen bonding density. However, there is still large room for improvement in the strength and toughness of ionogels based on previous findings. Therefore, we aim to enhance the strength and toughness of ionogels further by screening eutectic solvents and polymer monomers to increase the hydrogen bonding density within the ionogel.

In this study, we prepared ionogels by crosslinking *N*-hydroxyethylacrylamide (NHEMAA) in a DES composed of choline chloride (ChCl) and glycerol (Gly). The strong hydrogen bonding formed between the polymer chains and DES, as well as between the polymer chains themselves, contributed to the superior mechanical performances of the ionogels. The fracture stress of the ionogels could reach up to 11.44 MPa, while maintaining a fracture strain of 506% and a fracture energy of 27.29 MJ m^{-3}. By adjusting the content of NHEMAA, a wide range of mechanical performance of the ionogels could be achieved (fracture stress ranging from 0.3 MPa to 11.44 MPa and fracture strain ranging from 506% to 1050%). The mechanical properties of ChGly–NHEMAA ionogels are at a higher level compared to the ionogels reported so far, to the best of our knowledge. In addition, the ionogels also exhibit high ionic conductivity, visible light transparency (90%), excellent adhesion properties, and excellent frost resistance. This study provides a feasible method for the preparation of strong and tough ionogels, and their potential applications in the field of strain sensing are also demonstrated.

Experimental section

Materials

Acrylic acid (AA, 99%), *N*-hydroxyethylacrylamide (NHEMAA, 98%), hydroxyethyl acrylate (HEA, 99%), glycerol (Gly, 99%), urea (99%), ethylene glycol (EG, 98%), acetic acid (Ac, 99.5%), lactic acid (LA, 90%), choline chloride (Chcl, 98%), *N*,*N*′-methylenebisacrylamide (MBAA, 99%), and 2-hydroxy-4′-(2-hydroxyethoxy)-2-methylpropiophenone (Irgacure 2959, 98%) were purchased from Macklin Company.

Preparation of the DES

The hydrogen bond acceptor choline chloride (Chcl) and the hydrogen bond donor glycerol (Gly) were mixed in a molar ratio of 1 : 2. The mixture was then stirred and heated to 80 °C until complete dissolution to form a homogeneous solution. The solution was cooled to room temperature to obtain the DES. The preparation of other DES followed the same procedure.

Preparation of the ChGly–NHEMAA ionogels

To prepare 5 ml of the precursor solution, the required mass of monomers can be calculated based on the molar concentration of NHEMAA. Considering the similar densities of monomers and DES, any volume changes during the dissolution process can be neglected. Therefore, the volume of DES needed can be determined by the mass of monomers. The precursor solution is prepared by adding the crosslinking agent MBAA (C_{MBAA} = 0.1% mol, relative to NHEMAA) and the photoinitiator Irgacure 2959 (C_{MBAA} = 0.05% mol, relative to NHEMAA) to the mixture. The components are dispersed by stirring. The precursor solution is then poured into a mold and exposed to 365 nm ultraviolet light (approximately 50 mW cm^{-2}) for 5 minutes to form the ionogels. The preparation process for other ionogels follows the same procedure.

Testing and characterization

The optical properties of ChGly–NHEMAA ionogels were measured using a UV-visible spectrophotometer (Thermo Fisher Evolution 350) with a wavelength range of 250–900 nm. The Fourier-transform infrared (FTIR) spectroscopy of ChGly–NHEMAA ionogels in the wavelength range of 500–4000 cm^{-1} were recorded with a spectrometer (Nicolet iS 10). The ^1H NMR of ChGly–NHEMAA was analyzed and determined by Bruker AVANCE 600 MHz (Bruker Biospin Co., Ltd, Switzerland) spectrometer. The 30–50 mg sample was dissolved in 0.5 ml deuterated dimethyl sulfoxide, and the fully dissolved clarified sample was added to the washed and dried nuclear magnetic tube for determination at room temperature 600 MHz. Differential scanning calorimeter (DSC) measurements were conducted using a differential scanning calorimeter (Q100, TA Instruments) under a nitrogen atmosphere. The temperature range of the test was −60 °C to 30 °C, with a heating rate of 10 °C min^{-1}. Thermogravimetric analysis (TGA) was performed using a thermogravimetric analyzer to measure the thermal decomposition temperature of the ionogel. The temperature range of the test was 30 °C to 700 °C, with a heating rate of 10 °C min^{-1}.

The mechanical performance testing was conducted with a Ray Ran X350 universal testing machine at room temperature (25 °C). The test specimens were standard Type 2 dumbbell-shaped samples, and the tensile testing was performed at a speed of 100 mm min^{-1}. The tensile modulus of the ionogel was determined by taking the derivative of the stress–strain curve in the linear region, and the fracture energy of the ionogel was obtained by integrating the stress–strain curve. In the cyclic tensile testing, the testing machine applied a tensile speed of 50 mm min^{-1}.

The adhesion strength of the ionogels was investigated with a Ray Ran X350 Electro-mechanical Universal Testing Machines under room temperature (25 °C) conditions with a tensile speed of 10 mm min^{-1}. The substrates used were copper, aluminum, stainless steel, PVC, PMMA, PP, glass, and wood (100 mm × 25 mm × 2 mm in dimensions). Before conducting the shear test, the surface of the substrates was polished with sandpaper. Taking copper as an example, the tested ionogels were

compressed between two copper microscope slides measuring 12.5 mm × 25 mm × 0.5 mm.

The strain response of the ionogels was measured with an Electro-mechanical Universal Testing Machine in combination with a Keithley 2450 Digital Source Meter. Copper wires were used to connect the ionogels sensor to the circuit, and the real-time resistance of the ionogels sensor was tested using the Keithley 2450 Digital Source Meter. The tensile strain was controlled by the Electro-mechanical Universal Testing Machine. The assembled sensors were attached to different joints of the human body, such as the knee joint, wrist joint, elbow joint, *etc.*, to detect human motion signals. The relative resistance change ($\Delta R/R_0$) of the ionogels sensor was calculated with the following formula:

$$\frac{\Delta R}{R_0} = \frac{R - R_0}{R_0} \times 100\% \quad (1)$$

where R_0 and R represent the resistance at zero strain and under applied strain, respectively.

The conductivity of the tested samples was measured using an electrochemical workstation (CHI660E, Shanghai Chenhua Electronics Co., Ltd) by placing the circular-shaped ionogel samples on the test sample. The conductivity can be calculated with the following formula:

$$\sigma = \frac{I}{S \times R} \quad (2)$$

where I represents the thickness of the sample, S is the cross-sectional area of the sample, and R is the impedance value.

The weight retention of the sensors was determined by measuring their weight at different time intervals after placing them in a controlled environment at 25 °C and 20–40% RH for 12 days. The weight retention rate was calculated as the ratio of W_i to W_0, where W_0 represents the initial weight of the samples and W_i represents the weight of the ionogel samples after being placed at 25 °C and 30% RH for a specific number of days.

Results and discussion

The screening, synthesis, and characterization of ionogels

There are various types of deep eutectic solvents (DES). Considering the number of functional groups and relative molecular weight of hydrogen bond donors, we selected five hydrogen bond donors with higher hydrogen bond density: glycerol (Gly), ethylene glycol (EG), urea, acetic acid (Ac), and lactic acid (LA). These hydrogen bond donors were mixed with the hydrogen bond acceptor, choline chloride (Chcl), to prepare five different DES. Through preliminary screening, we identified three polymer monomers which can form hydrogen bonding with DES and exhibit good compatibility: acrylic acid (AA), hydroxyethyl acrylate (HEA), and *N*-hydroxyethyl methacrylamide (NHEMAA). Ionogels were prepared by combining the monomers with DES, generating 15 different systems. The ionogel preparation process is illustrated in Fig. 1a. The monomers, crosslinking agent, and photo-initiator were dissolved in DES. ^{1}H NMR of the precursor solution showed that no other reaction occurred before initiating polymerization, as shown in Fig. S1.† The mixed solution was then exposed to ultraviolet (UV) light. The monomers underwent free radical polymerization, forming a uniformly distributed polymer network upon the linkage of the crosslinking agent. Simultaneously, high-density hydrogen bonding was formed between polymer chains, as well as between polymer chains and the solvent, leading to the rapid gelation of the precursor solution.

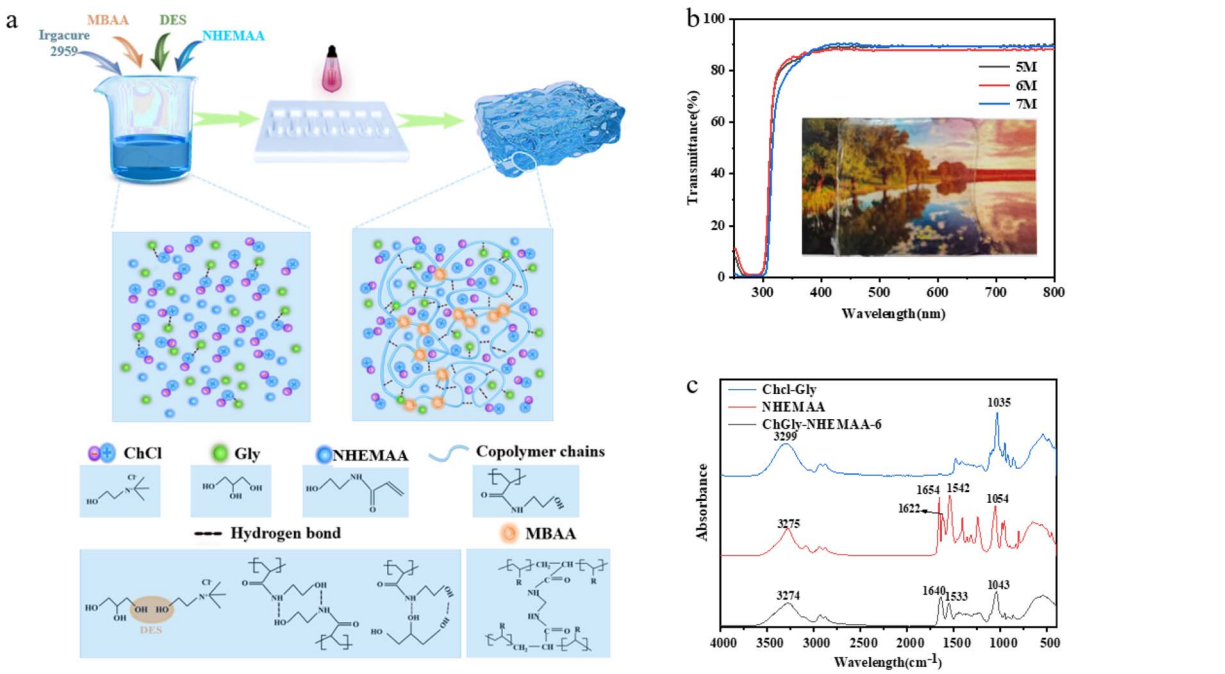

Fig. 1 (a) Preparation process and internal structure of ionogel, (b) light transmittance test of ChGly–NHEMAA ionogel; (c) infrared spectrum of ChCGly, NHEMAA and ChGly–NHEMAA-6.

As an example, ionogels prepared using Chcl and Gly-based DES with NHEMAA were named ChGly–NHEMAA-*x*, where *x* represents the molar concentration of the monomers.

Due to the presence of a uniformly dispersed polymer network structure, the prepared ionogels exhibited high visible light transmittance. Taking the ChGly–NHEMAA system as an example, as shown in Fig. 1b, the photo behind a 1 mm-thick ChGly–NHEMAA-6 ionogel was clearly visible. Quantitative measurements of the transparency of ChGly–NHEMAA ionogels showed that they exhibited approximately 90% transmittance in the wavelength range of 400 nm to 800 nm. The infrared spectra of ChGly, NHEMAA, and ChGly–NHEMAA-6 are shown in Fig. 1c. ChGly exhibits a broad absorption peak in the range of 3200 cm^{-1} to 3500 cm^{-1}, attributed to the intermolecular hydrogen bonding of –OH groups. NHEMAA shows a broad peak at 3275 cm^{-1}, which corresponds to the stretching vibration of –OH and –NH– groups. However, in ChGly–NHEMAA-6, the stretching vibration peaks of –OH and –NH– shift to 3274 cm^{-1} due to the mutual interaction between hydrogen bonds in the ionogel. The stretching vibration peak of –C═O at 1654 cm^{-1} also exhibits a similar shift. The bending vibration of –N–H– in the ionogel corresponds to the peak at 1533 cm^{-1}. The stretching vibration peak of –C═C– in NHEMAA is observed at 1622 cm^{-1}, and its disappearance in the ionogel indicates the copolymerization of NHEMAA. The FTIR results suggest that ChGly–NHEMAA-6 is composed of both covalent bonds and hydrogen bond networks.

Mechanical properties of ionogels

The 15 different ionogels prepared with high-density hydrogen bonding exhibit excellent mechanical properties. The stress–strain curves of the ionogels at different solute concentrations

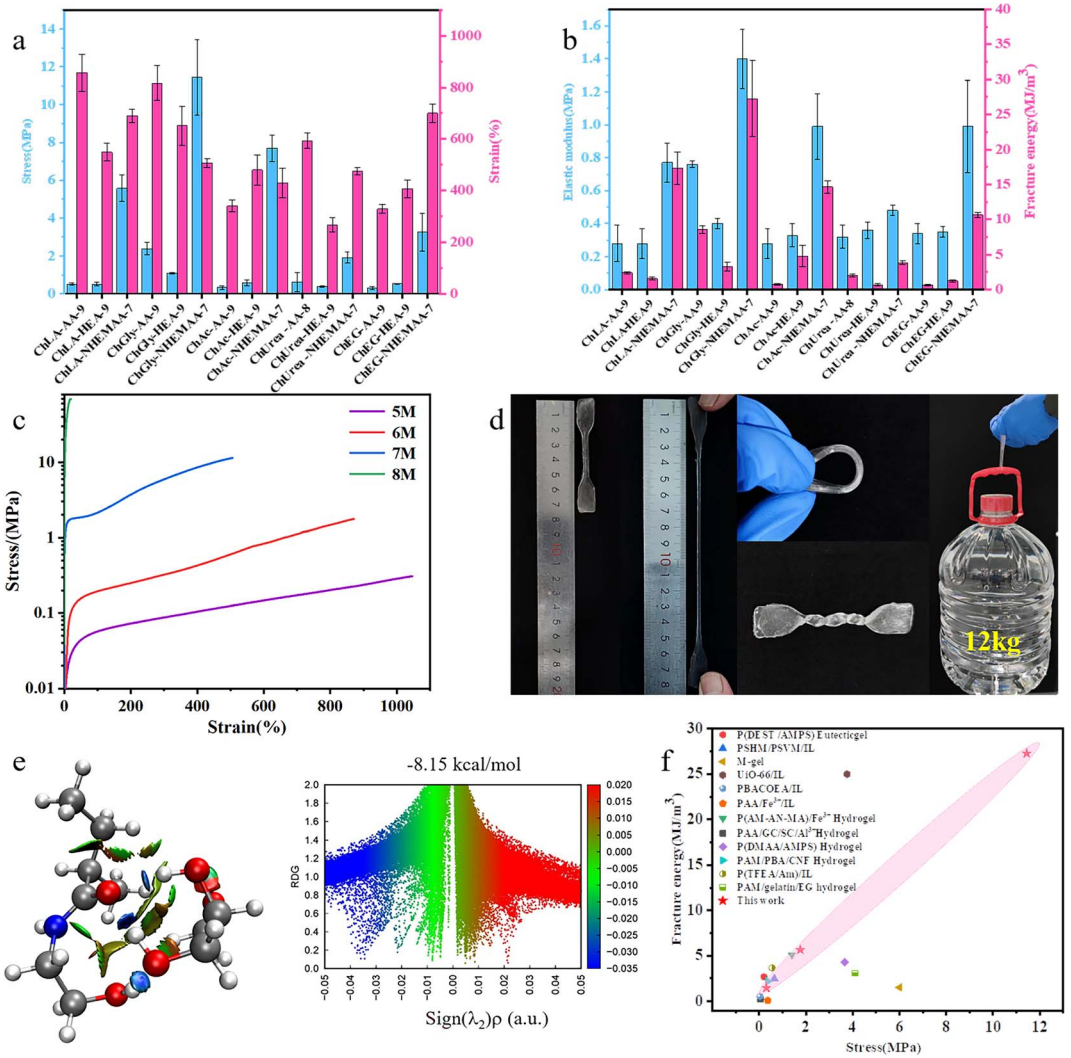

Fig. 2 (a) Fracture stress and fracture strain of 15 ionogel with the best performance; (b) the breaking energy and tensile modulus of 15 kinds of best performance ionogel; (c) stress–strain curve of ionogel of ChGly–NHEMAA system, the tensile speed is 100 mm min^{-1}; (d) schematic diagram of ChGly–NHEMAA-7 ionogel stretching, bending, twisting and lifting 12 kg weight; (e) color filled RDG images of Gly and NHEMAA (isovalue = 0.5) and RDG *versus* sign(λ_2)ρ for the synthetic DEST, respectively, where the sign(λ_2)ρ ranges from −0.05 to 0.05. The color bar shows that blue, green, and red represent strong attraction interactions (hydrogen bonding), van der Waals interactions, and strong nonbonded overlap, respectively; (f) comparison of fracture stress and toughness between ChGly–NHEMAA and other reported ionogels.

are shown in Fig. S2, ESI.† From the curves, it can be observed that as the solute concentration increases, the fracture strength, tensile modulus, and fracture energy of the ionogels all increase. This is mainly attributed to the increase in polymer crosslinking density. The optimal compositions of fracture stress and fracture strain for each system's mechanical performance are shown in Fig. 2a, and the tensile modulus and fracture energy of the ionogels are calculated based on the stress–strain curves (Fig. 2b).

Comparing the mechanical properties of ionogels composed of different monomers within the same DES, it is evident that the ionogel formed by NHEMAA at a monomer concentration of 7 M exhibits significantly higher fracture strength and fracture toughness compared to the ionogels prepared with AA and HEA at a concentrations of 9 M. For example, in the ChGly DES system, the fracture strength and fracture energy of ChGly–NHEMAA-7 are 11.438 MPa and 27.294 MJ m^{-3}, respectively, while ChGly–AA-9 only has a fracture strength of 2.38 MPa and a fracture energy of 8.55 MJ m^{-3}. The performance of ChGly–HEA-9 is even poorer. Firstly, NHEMAA possesses a higher number of hydrogen bonding sites, allowing it to form hydrogen bonds with a higher density after polymerization. Additionally, NHEMAA has a higher relative molecular weight than AA, which means longer polymer chains and increased entanglement between the chains after polymerization. This higher degree of entanglement makes it more difficult for the polymer chains to move upon stress. The main difference between NHEMAA and HEA lies in the fact that the amide groups in NHEMAA act as both electron-donating and electron-withdrawing groups, while the ester groups in HEA only act as electron-withdrawing groups. This difference results in a higher density of hydrogen bonding in NHEMAA and makes it more prone to forming hydrogen bonds and entangling with neighboring polymer chains.[27–30] Therefore, ionogels composed of NHEMAA exhibit superior mechanical performance compared to those composed of HEA.

Comparing ionogels prepared with the same monomers and concentration but different DES, it can be observed that ionogels prepared with Gly and Chcl based DES exhibit higher mechanical performance. For instance, in ionogels prepared with AA as the matrix, the fracture strength of ChGly–AA-9 is 2.38 MPa, whereas the fracture strengths of ChLA–AA-9, ChAC–AA-9, ChUrea–AA-8, and ChEG–AA-9 are significantly lower, which are only 0.507 MPa, 0.326 MPa, 0.616 MPa, and 0.453 MPa, respectively. Moreover, the fracture energy of ChGly–AA-9 exceeds those of ionogels in other solvents. This is attributed to the higher hydrogen bonding density in the Chcl–Gly DES system. Additionally, subsequent RDG simulation calculations indicate that the hydrogen bonding energy between Gly molecules and the polymer is higher.

It is evident from the test results that the ChGly–NHEMAA system exhibits significantly higher mechanical performance compared to other ionogels at the same concentration. Fig. 2c shows the stress–strain curves of the ChGly–NHEMAA system. When the monomer concentration of NHEMAA is 8 M, the ionogel becomes stiff and brittle, with a fracture stress of 68.6 MPa. However, the fracture strain is only 19.53%, indicating a high density of entangled branches.[31] At higher concentrations, the samples experience brittle fracture during the demolding process and are not practically useful. At a concentration of 7 M, the ionogel exhibits optimal mechanical performance, with a fracture stress of 11.438 MPa and a fracture energy of 27.294 MJ m^{-3}. Additionally, the ionogel maintains a high elongation at break of 506%. This performance surpasses the majority of reported ionogels to date. Fig. 2d shows the image of the ChGly–NHEMAA-7 ionogel, demonstrating its excellent deformability in terms of stretching, bending, and twisting, *etc.* (Fig. 2d). The ionogel can even easily lift a 12 l bottle of mineral water. Furthermore, as the solute content decreases, the ChGly–NHEMAA ionogel exhibits a wide range of mechanical performance adjustments. The fracture stress of ChGly–NHEMAA-6 is 1.76 MPa, while the fracture stress of ChGly–NHEMAA-5 decreases to 0.308 MPa, with a corresponding fracture strain of 1050.04%. This wide range of mechanical performance adjustments expands the application potential of the ionogels. Regarding ChGly–NHEMAA-5 and ChGly–NHEMAA-6, their moduli closely resemble human skin, making them suitable for applications in flexible strain sensors, such as electronic skins, soft robotics.[32,33] Additionally, due to their high modulus and strength, ChGly–NHEMAA-5 can be utilized as an electrolyte in lithium-ion batteries to suppress the growth of lithium dendrites and enhance the device's resistance to external impacts, thereby alleviating safety concerns associated with short circuits.[34,35]

To investigate the hydrogen bonding within the ionogel further quantitatively, we calculated the hydrogen bonding energies between different solvent molecules and polymer monomers, as shown in Fig. 2e. We also generated color-filled Reduced Density Gradient (RDG) plots. Fig. 2e specifically depicts the interaction between Gly molecules and NHEMAA, with a binding energy of −8.15 kcal mol^{-1}. For the remaining calculation results, please refer to Fig. S3, ESI.† The calculated results indicate that the binding energy between Gly and NHEMAA is significantly higher than that between the other solvent molecules and polymer monomers. This finding explains the excellent mechanical performance observed in the ChGly–NHEMAA ionogel system. Furthermore, the fracture strength and fracture energy of the ionogel show a positive correlation with the hydrogen bonding energies between solvent molecules and monomers. This validates the feasibility of our concept to design tough ionogels by constructing high-density hydrogen bonding systems.

We also performed cyclic stress–strain curves on the ChGly–NHEMAA ionogel system under a 200% strain for 10 consecutive cycles (Fig. S4†). The residual strain after 10 cycles increased with the increasing polymer component contents: 13.57% for ChGly–NHEMAA-5, 26.18% for ChGly–NHEMAA-6, and 89.37% for ChGly–NHEMAA-7. This behavior can be attributed to the entanglement between polymer chains. ChGly–NHEMAA-5 and ChGly–NHEMAA-6 exhibited excellent recovery rates. ChGly–NHEMAA-7, with a lower solvent content, exhibited a larger hysteresis due to increased resistance to polymer chain displacement. However, it still achieved full recovery to its original length within 3 minutes. The remarkable recovery

performance of the ChGly–NHEMAA ionogel system highlights its potential application in the field of flexible strain sensing.

Fig. 2f illustrates a comparison of the maximum fracture stress and fracture energy among typical ionogels reported to date. It is evident that the mechanical performance of ChGly–NHEMAA ionogels surpasses the majority of the reported ionogels and hydrogels. These include poly(AA)/acrylated cytosine (Ca)–acrylated guanine (Ga)/sodium caseinate (SC)/Al^{3+} ionogel,[36] poly(deep eutectic solvent mixture (DEST)/2-acrylamido-2-methyl-1-propanesulfonic (AMPS)) eutectic gel,[27] poly(*tert*-butyl styrene-*block*-(4-hydroxystyrene-random-methyl acrylate)) (PSHM)/poly(*tert*-butyl styrene-*block*-(2-vinyl pyridine-random-methyl acrylate)) (PSVM)/[EMI][TFSI] (IL) ionogel,[37] poly(-acrylamide (AM)–acrylonitrile (AN)–maleic acid (MA))/Fe^{3+} hydrogel,[38] poly(*N*,*N*-dimethylacrylamide (DAAM)/2-acrylamido-2-methylpropane-sulfonic acid (AMPS)) hydrogel,[39] multiscale-structured ionogel (M-gel),[40] PAM/4-(bromomethyl) phenylboronic acid-1-vinylimidazole (PBA)/cellulose nanofibrils (CNF) hydrogels,[41] PDMAA/Zr-MOF (Zr-metal–organic frameworks)/IL (UiO-66) ionogel,[42] poly(2,2,2-trifluoroethyl acrylate (TFEA)–AM)/IL ionogel,[43] PAA/Fe^{3+}/IL ionogel,[44] poly 2-[[(butylamino)carbonyl]oxy]ethyl acrylate (PBACOEA)/IL ionogel,[45] PAM/gelatin/EG hydrogel.[46] Additionally, the figure highlights the wide range of mechanical property tuning achievable in the ChGly–NHEMAA system. These all benefit from the high density and adjustable hydrogen bonding cross-linking network inside the ChGly–NHEMAA system.

Adhesion performance of the ionogels

When used as wearable flexible strain sensing devices, the adhesion of ionogels to substrates is crucial for ensuring reliable signal acquisition. We evaluated the adhesion strength of the ChGly–NHEMAA system to eight common materials (aluminum, polypropylene, stainless steel, polytetrafluoroethylene, polyvinyl chloride, glass, wood, and copper) through shear adhesion test, as schematically shown in Fig. 3a. Due to the abundant non-covalent interactions between the ionogel and the substrates, the ionogel exhibited strong adhesion to all eight substrates, capable of easily lifting a 1 kg weight, as depicted in Fig. 3b.

Among them, ChGly–NHEMAA-7 exhibited the highest adhesion strength to wood, reaching 413.9 kPa (Fig. 3c). It is attributed to the presence of abundant hydrogen bonding within the ionogel, which can also form a high-density hydrogen bonding network with the cellulose in wood. The ionogel also demonstrated strong adhesion to metals. This may be due to the presence of a large number of free chloride ions in the ionogel, which can form electrostatic interactions with metal cations. Additionally, it is evident that the adhesion strength of the ionogel significantly increases with the increase of polymer content. This is because the adhesion strength of the

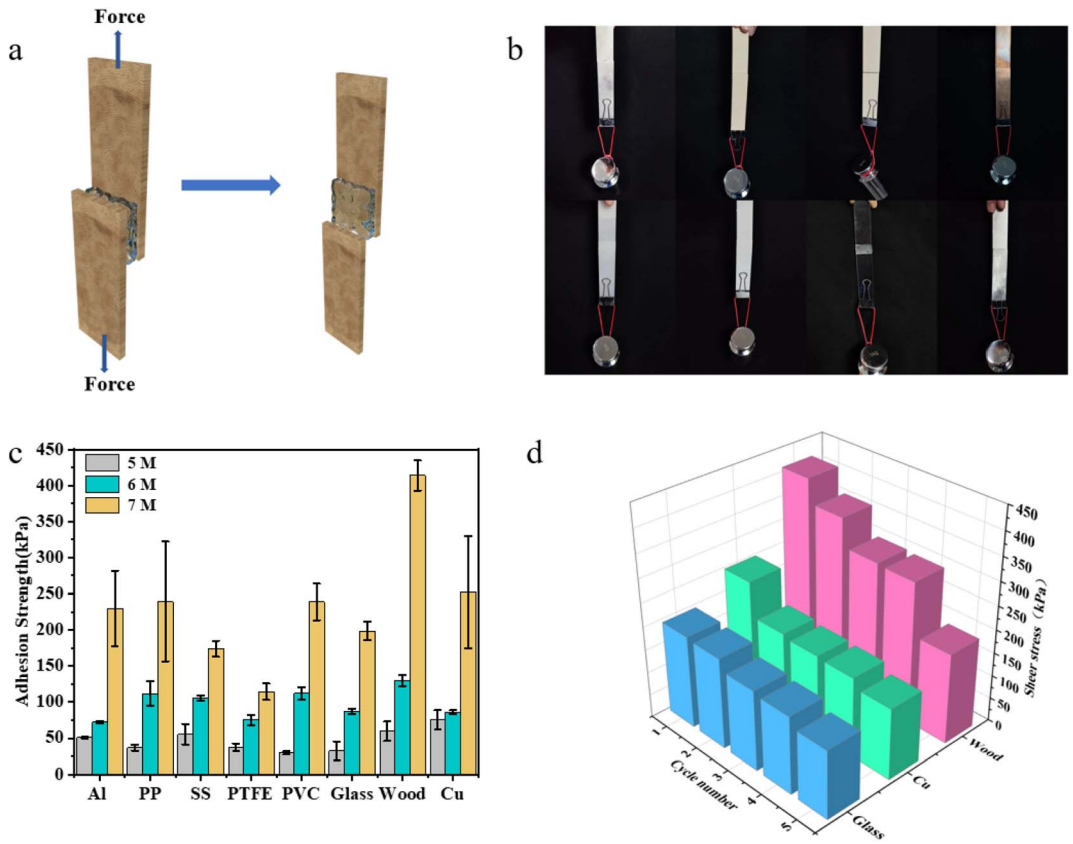

Fig. 3 (a) Schematic diagram of ionogel lap shear test, the tensile speed is 10 mm min^{-1}; (b) demonstration of the adhesion performance of ionogel on different substrates; (c) adhesion strength of ChGly–NHEMAA ionogel on different substrates; (d) adhesion strength of ChGly–NHEMAA-7 ionogel to wood, copper and glass for 5 consecutive lap shear joints.

ionogel is not only influenced by the surface interactions between the ionogel and the substrate but also correlated with the ionogel's strength and toughness.[47] Moreover, the ionogel exhibits excellent repeatability in adhesive performance (Fig. 3d). We conducted continuous adhesion-peeling tests on glass, wood, and copper surfaces to evaluate the adhesion strength. It can be observed that the adhesion strength of the ionogel slightly decreases with an increasing number of cycles, but it still maintains excellent adhesion (above 150 kPa after 5 cycles). The decrease in adhesion strength may be attributed to the residual ionogel on the substrate surface and the reduction in strength due to tearing of the ionogel.

Environmental stability and shape memory capability of the ionogels

Excellent environmental stability is essential for sensors to maintain stable operation. Traditional hydrogels often suffer from gel failure due to high-temperature evaporation and low-temperature crystallization of water, which severely limits their practical applications. However, ionogels prepared using DES exhibit superior environmental stability due to their high-density internal hydrogen bonding and low melting point, as well as their resistance to volatilization. The solidification point of the ChGly–NHEMAA system was determined with differential scanning calorimeter (DSC), as shown in Fig. 4a. When water was used as a substitute for DES to prepare the hydrogel, it can be seen from the figure that the hydrogel in the control group has obvious exothermic peak due to water crystallization at $T = -7.83$ °C, while the DSC test curves of ChGly–NHEMAA ionogels have no obvious peak or step-like change in the range of −60 °C to 30 °C. This shows that ChGly–NHEMAA gels have excellent stability compared with hydrogels in low temperature environments. Even after being stored at −20 °C for 24 hours, the ChGly–NHEMAA ionogel still maintained excellent elasticity and could be bent, twisted, as demonstrated by its stress–strain curve (Fig. S5†). The comparison of the mechanical performance at room temperature and after freezing reveals a significant improvement in fracture stress and fracture energy of the ionogel. After freezing, ChGly–NHEMAA-7 exhibited a fracture stress of 13.09 MPa (Fig. 4d) and a fracture energy of 41.07 MJ m^{-3} (Fig. 4e), representing a 1.5-fold increase. These results demonstrate the excellent low-temperature stability of the ChGly–NHEMAA system, which exhibits enhanced mechanical performance at lower temperatures. This enhancement can be attributed to the suppression of molecular thermal motion at low temperature, improving the stability of hydrogen bonds.

Thermogravimetric analysis (TGA) was conducted to determine the thermal decomposition temperature of the ionogels (Fig. 4b). The $T5\%$ thermal decomposition temperature of hydrogel, ChGly–NHEMAA-5, ChGly–NHEMAA-6 and ChGly–NHEMAA-7 is 74.6667 °C, 159.833 °C, 222.167 °C and 199.833 °C, respectively. Compared with hydrogels, the $T5\%$ thermal decomposition temperature of ChGly–NHEMAA ionogels is more than doubled, which indicates that ChGly–NHEMAA gels have excellent high-temperature stability and will not fail due to the evaporation of solvents at room temperature or higher temperatures. We also conducted a mass residue rate test on the ionogels under constant temperature (25 °C) and humidity (20% to 40%) conditions (Fig. 4c). The hydrogels experienced significant dehydration and exhibited volume shrinkage and increased stiffness after 12 days of storage. On the other hand,

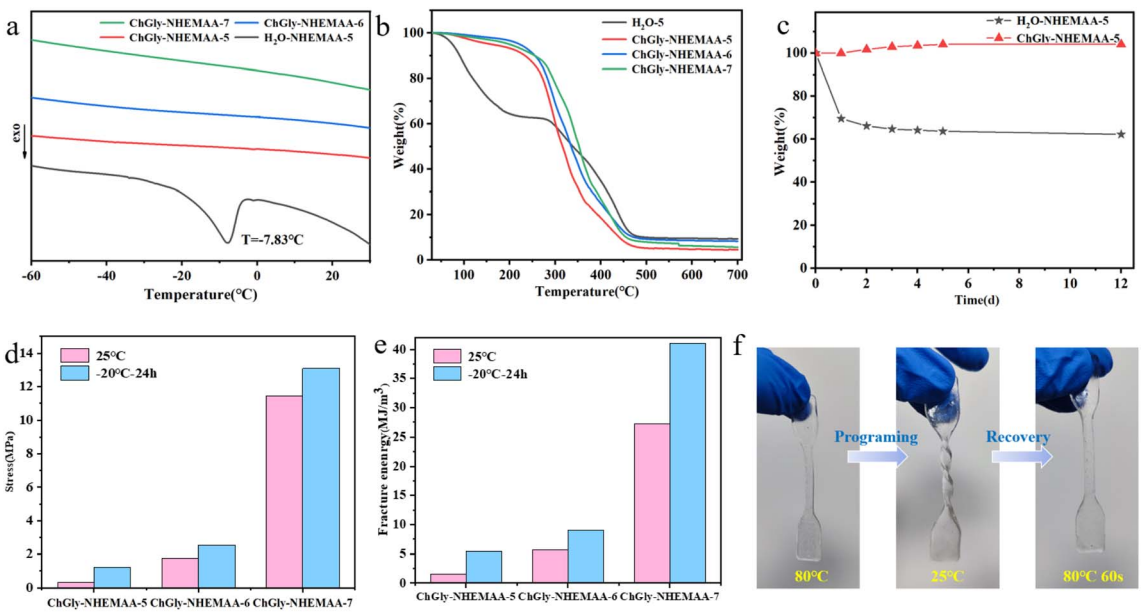

Fig. 4 (a) DSC test results of ChGly–NHEMAA ionogel and hydrogel; (b) TG test results of ChGly NHEMAA ionogel and hydrogel; (c) mass changes of ChGly–NHEMAA-5 and H_2O–NHEMAA-5 after 12 days of storage; (d) comparison of the fracture stress of ChGly–NHEMAA ionogel at room temperature and after freezing at −20 °C for 24 h; (e) comparison of fracture energy between ChGly–NHEMAA at room temperature and frozen at −20 °C for 24 hours; (f) display of shape memory ability of ChGly–NHEMAA-7 ionogel.

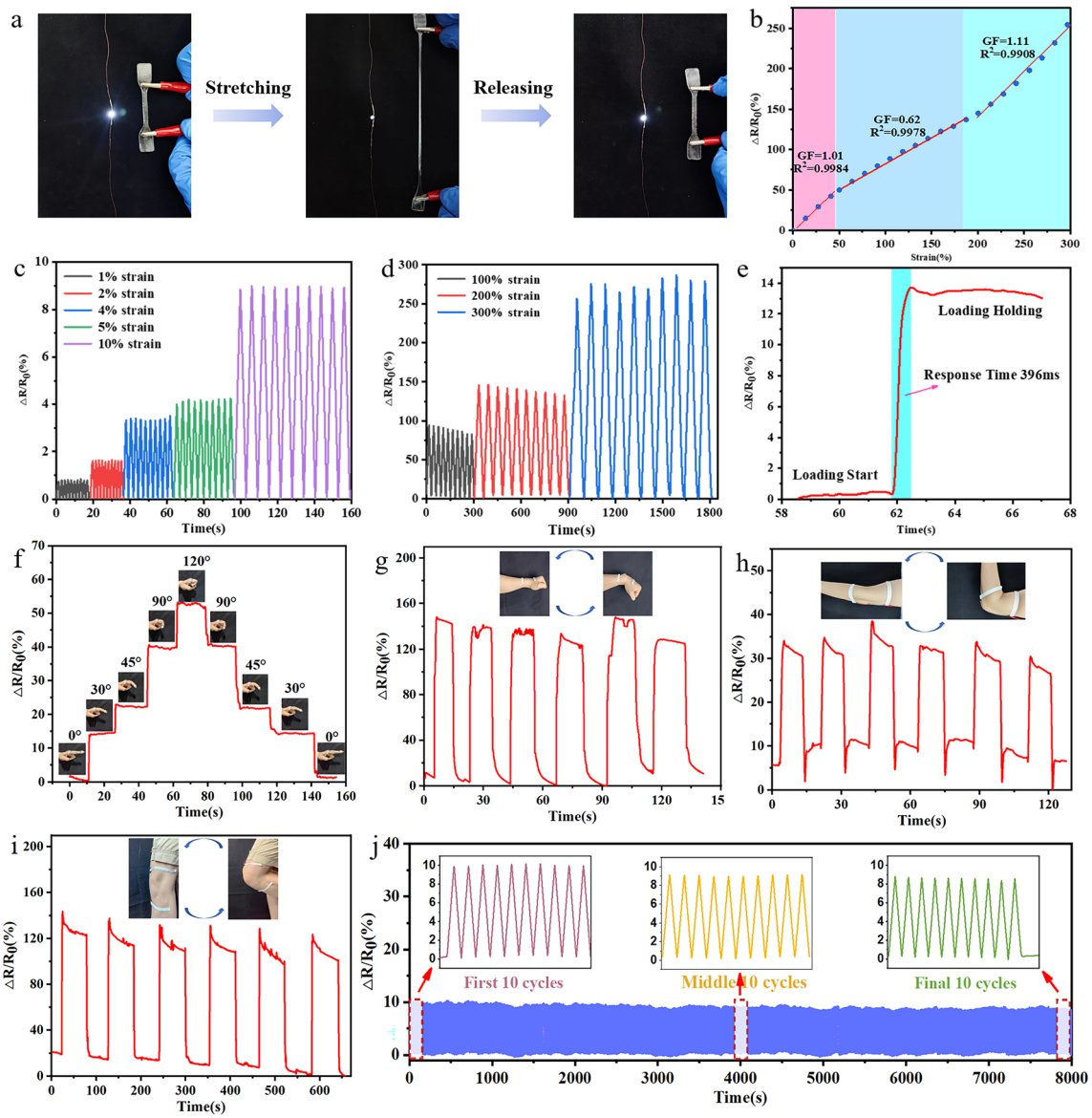

Fig. 5 (a) Sensing demonstration of ChGly–NHEMAA ionogel; (b) change of relative resistance and corresponding GF value of ChGly–NHEMAA-6 ionogel under 300% strain; (c) the change of relative resistance of ionogel under cyclic tension in the strain range of 1–10%; (d) the change of relative resistance of ionogel under cyclic tension in the strain range of 100–300%; (e) response time test of ionogel; monitor four continuous motion joints: (f) fingers, (g) wrists, (h) elbows, and (i) knees; (j) the change of relative resistance of ionogel after 1000 cycles of stretching under 50% strain.

the ChGly–NHEMAA ionogel showed no significant changes in mass during the same period.

Ionogels demonstrate excellent shape memory capability due to the presence of numerous dynamic bonds within the ionogel structure (Fig. 4f). The shape memory ability of ionogels is achieved through a process called thermal programming, during which the ionogel is heated to a high temperature to induce a desired shape ("programming"), and then cooled to retain the programmed shape. Upon reheating, the ionogel is capable of recovering its original shape. For example, an ionogel in the shape of a dumbbell can be twisted into a helical shape at a high temperature (80 °C). After cooling to room temperature, the ionogel retains the helical shape. When heated again to 80 °C, the ionogel undergoes shape recovery and returns to its original shape within 30 seconds. The shape memory capability of the ionogel is attributed to the high-temperature breakage and low-temperature reformation of hydrogen bonds within the ionogel structure. During the cooling process after programming, the formation of a large number of hydrogen bonds increases the ionogel modulus, resulting in a hardened state that maintains the programmed shape. Upon reheating, the hydrogen bonds break, providing the driving force for the softening of the covalently cross-linked network, thus enabling the ionogel to recover its original shape.

Application in strain sensors

Increasing the modulus and strength of the ionogel can improve the sensitivity and damage resistance of flexible sensors. ChGly–NHEMAA ionogel contains a large number of Cl^- ions, which endow the ionogel with excellent ionic conductivity. The ionic conductivity of ChGly–NHEMAA-5, ChGly–NHEMAA-6, and ChGly–NHEMAA-7 at 25 °C are 2.27×10^{-4} S m^{-1}, 0.79×10^{-4} S m^{-1}, and 0.31×10^{-5} S m^{-1}, respectively. The excellent conductivity, deformability, and environmental stability of the ionogel make it highly promising for applications in the field of flexible sensors. Taking into account of the ionogel's mechanical performance and deformation recovery rates, we chose to use ChGly–NHEMAA-6 to fabricate a simple strain sensor device and investigate its sensing performance.

The ionogels are connected to a circuit that includes an LED light. When the circuit is powered on, the brightness of the LED light decreases as the ionogel is stretched, and when the ionogel returns to its original length, the LED light becomes bright again (Fig. 5a). It demonstrates that the strain sensors have good strain-responsive behavior. Sensitivity is a key parameter for evaluating sensing performance. The sensitivity of the ChGly–NHEMAA ionogel is measured by calculating the slope of the relative change in resistance $(R - R_0)/R_0$ with respect to the strain curve, resulting in the gauge factor (GF), as shown in Fig. 5b. The GF values of the ionogel can be roughly divided into three linear response regions: 0–50% strain with GF = 1.01, 50–200% strain with GF = 0.62, and 200–300% strain with GF = 1.11. It indicates that the ionogel exhibits excellent sensing sensitivity within the 300% strain range. Additionally, the response time of the ionogel was measured to be 396 ms, demonstrating its outstanding sensing performance (Fig. 5e). Furthermore, from Fig. 5c and d, it can be observed that the ionogel exhibits stable signal output in both small strain conditions (1–10%) and large strain conditions (100–300%). The cyclic stability of the sensor device is crucial for its practical applications. We conducted a continuous 1000-cycle signal output test on the ionogel at 50% strain, as shown in Fig. 5j. It can be observed that during the 1000 cycles, the resistance signal maintains a stable waveform and amplitude, demonstrating the excellent cyclic stability of the ionogel. As a wearable strain sensing device, the ionogel can monitor the movements of human joints (fingers, wrists, elbows, and knees), as shown in Fig. 5f–i. For different degrees of bending in finger joints, the ionogel can generate corresponding resistance signals with distinct recognizability, meeting the requirements for daily human motion monitoring.

Conclusion

In summary, we have proposed a simple method for the preparation of strong and tough ionogels. By constructing a high-density hydrogen bond network within the ionogel, the ionogels exhibit a maximum fracture strength of 11.44 MPa, while maintaining a high stretchability of 506% and a fracture energy of 27.294 MJ m^{-3}. By adjusting the content of monomers, it is possible to achieve a wide range tuning of the ionogel's mechanical performance. Additionally, the ionogel exhibits high transparency (90%), high ion conductivity, frost resistance, as well as excellent adhesion and shape memory capabilities. In addition, the flexible strain sensor devices fabricated from ionogels through a simple installation process demonstrate high sensitivity (GF = 1.01), fast response (396 ms), and excellent cyclic stability. They can enable real-time monitoring of human joint movements, making them highly promising for applications in flexible wearable devices. Ultimately, our work validates the feasibility of achieving strong and tough ionogels through the construction of a high-density hydrogen bonding network, providing new insights into the design and fabrication of ionogels.

Conflicts of interest

There are no conflicts to declare.

References

1 Z. Liu, Y. Wang, Y. Ren, G. Jin, C. Zhang, W. Chen and F. Yan, *Mater. Horiz.*, 2020, **7**(3), 919–927.
2 Y. Ye, H. Oguzlu, J. Zhu, P. Zhu, P. Yang, Y. Zhu, Z. Wan, O. J. Rojas and F. Jiang, *Adv. Funct. Mater.*, 2023, **33**(2), 2209787.
3 L. Zhang, Y. He, S. Cheng, S. Sheng, K. Dai, W. Zheng, M. Wang, Z. Chen, Y. Chen and Z. Suo, *Small*, 2019, **15**(21), e1804651.
4 J. Tie, Z. Mao, L. Zhang, Y. Zhong, X. Sui and H. Xu, *Sci. China Mater.*, 2023, **66**(5), 1899–1910.
5 Y. Xu, L. Chen, J. Chen, X. Chang and Y. Zhu, *ACS Appl. Mater. Interfaces*, 2021, **14**(1), 2122–2131.
6 Q. Xia, W. Li, X. Zou, S. Zheng, Z. Liu, L. Li and F. Yan, *Mater. Horiz.*, 2022, **9**(11), 2881–2892.
7 H. Cheng, X. He, Z. Fan and J. Ouyang, *Adv. Energy Mater.*, 2019, **9**(32), 1901085.
8 Z. Li, J. Wang, R. Hu, C. Lyu and J. Zheng, *Macromol. Rapid Commun.*, 2019, **40**(7), 1800776.
9 J. H. Kwon, Y. M. Kim and H. C. Moon, *ACS Appl. Mater. Interfaces*, 2022, **14**(28), 32533–32540.
10 A. Hu, C. Liu, Z. Cui, Z. Cong and J. Niu, *ACS Appl. Mater. Interfaces*, 2022, **14**(10), 12713–12721.
11 B. He, Y. Zhou, Z. Wang, Q. Wang, R. Shen and S. Wu, *Sens. Actuators, A*, 2018, **272**, 341–348.
12 G. Ge, K. Mandal, R. Haghniaz, M. Li, X. Xiao, L. Carlson, V. Jucaud, M. R. Dokmeci, G. W. Ho and A. Khademhossini, *Adv. Funct. Mater.*, 2023, **33**(9), 2207388.
13 Y. Ren, J. Guo, Z. Liu, Z. Sun, Y. Wu, L. Liu and F. Yan, *Sci. Adv.*, 2019, **5**(8), eaax0648.
14 Z. Lei and P. Wu, *Nat. Commun.*, 2019, **10**(1), 3429.
15 X. Fan, S. Liu, Z. Jia, J. J. Koh, J. C. C. Yeo, C. Wang, N. E. Surat, X. J. Loh, J. L. Bideau, C. He, Z. Li and T. Loh, *Chem. Soc. Rev.*, 2023, **52**(7), 2497–2527.
16 W. Li, L. Li, S. Zheng, Z. Liu, X. Zou, Z. Sun, J. Guo and F. Yan, *Adv. Mater.*, 2022, **34**(28), 2203049.

17 W. Li, S. Zheng, X. Zou, Y. Ren, Z. Liu, W. Peng, X. Wang, D. Liu, Z. Shen, Y. Hu, J. Guo, Z. Sun and F. Yan, *Adv. Funct. Mater.*, 2022, **32**(43), 2207348.
18 X. Zhao, S. Guo, H. Li, J. Liu, C. Su and H. Song, *RSC Adv.*, 2017, **7**(61), 38765–38772.
19 J. Liu, H. Song, Z. Wang, J. Zhang and X. Ba, *J. Mater. Sci.*, 2020, **55**(9), 3991–4004.
20 Q. Lv, X. Sun, L. Ye and H. Liang, *J. Mater. Chem. B*, 2022, **10**(16), 3126–3137.
21 A. Kang, C. Liu, Z. Cui, Z. Cong and J. Niu, *ACS Appl. Mater. Interfaces*, 2022, **14**(10), 12713–12721.
22 B. B. Hansen, S. Spittle, B. Chen, D. Poe, Y. Zhang, J. M. Klein, A. Horton, L. Adhikar, T. Zelovich, B. W. Doherty, B. Gurkan, E. J. Maginn, A. Ragauskas, M. Dadmun, T. A. Zawodzinski, G. A. Baker, M. E. Tuckerman, R. F. Savinell and J. R. Sangoro, *Chem. Rev.*, 2020, **121**(3), 1232–1285.
23 C. Ruß and B. König, *Green Chem.*, 2012, **14**(11), 2969–2982.
24 L. C. Tomé and D. Mecerreyes, *J. Phys. Chem. B*, 2020, **124**(39), 8465–8478.
25 Q. Zhang, G. Chen, R. Li, L. Lin and M. He, *Polym. Chem.*, 2021, **12**(13), 2016–2023.
26 R. Wang, P. Chen, X. Zhou, L. Sun, G. Wang, Y. Liu and C. Gao, *Adv. Mater. Technol.*, 2023, **8**(7), 2201509.
27 D. Zhang, Z. Xu, H. Li, C. Fan, C. Cui, T. Wu, M. Xiao, Y. Yang, J. Yang and W. Liu, *Biomater. Sci.*, 2020, **8**(5), 1455–1463.
28 D. Zhang, Y. Tang, Y. Zhang, F. Yang, Y. Liu, X. Wang, J. Yang, X. Gong and J. Zheng, *J. Mater. Chem. A*, 2020, **8**(39), 20474–20485.
29 H. Chen, Y. Liu, B. Ren, Y. Zhang, J. Ma, L. Xu, Q. Chen and J. Zheng, *Adv. Funct. Mater.*, 2017, **27**(44), 1703086.
30 Y. Zhang, J. Xue, D. Li, Z. Huang, Y. Huang, C. Gong, S. Long and X. Li, *Polym. Test.*, 2021, **93**, 106976.
31 J. Xu, Z. Guo, Y. Chen, Y. Luo, S. Xie, Y. Zhang, H. Tan, L. Xu and J. Zheng, *Polymer*, 2021, **236**, 124321.
32 J. Kim, J. W. Kim, K. Keum, H. Lee, G. Jung, M. Park, Y. H. Lee, S. Kim and J. S. Ha, *Chem. Eng. J.*, 2023, 141278.
33 X. Zhao, J. Xu, J. Zhang, M. Guo, Z. Wu, Y. Li, C. Xu, H. Yin and X. Wang, *Mater. Horiz.*, 2023, **10**(2), 646–656.
34 I. Osada, H. de Vries, B. Scrosati and S. Passerini, *Angew. Chem., Int. Ed.*, 2016, **55**(2), 500–513.
35 N. Chen, H. Zhang, L. Li, R. Chen and S. Guo, *Adv. Energy Mater.*, 2018, **8**(12), 1702675.
36 B. Kang, M. Gao, R. Zhao, Z. Zhao and S. Song, *Polymer*, 2023, **272**, 125844.
37 K. G. Cho, S. An, D. H. Cho, J. H. Kim, J. Nam, M. Kim and K. H. Lee, *Adv. Funct. Mater.*, 2021, **31**(36), 2102386.
38 Y. Wang, Y. Xie, X. Xie, D. Wu, H. Wu, X. Luo, Q. Wu, L. Zhao and J. Wu, *Adv. Funct. Mater.*, 2023, 2210224.
39 C. Fu, L. Liang, H. Zhong, W. Shan, P. Liu and T. Q. Bui, *Polymer*, 2023, **272**, 125834.
40 K. Cao, Y. Zhu, Z. Zheng, W. Chen, Y. Zi, S. Zeng, D. Zhao and D. Yu, *Adv. Sci.*, 2023, **10**(13), 2207233.
41 X. Yao, S. Zhang, L. Qian, N. Wei, V. Nica, S. Coseri and F. Han, *Adv. Funct. Mater.*, 2022, **32**(33), 2204565.
42 Q. Xia, W. Li, X. Zou, S. Zheng, Z. Liu, L. Li and F. Yan, *Mater. Horiz.*, 2022, **9**(11), 2881–2892.
43 L. Xu, Z. Huang, Z. Deng, Z. Du, T. Sun, Z. Guo and K. Yue, *Adv. Mater.*, 2021, **33**(51), 2105306.
44 Y. Wang, Y. Liu, N. Hu, P. Shi, C. Zhang and T. Liu, *Sci. China Mater.*, 2022, **65**(8), 2252–2261.
45 A. Hu, C. Liu, Z. Cui, Z. Cong and J. Niu, *ACS Appl. Mater. Interfaces*, 2022, **14**(10), 12713–12721.
46 S. Liu, Y. Chen, J. Feng, J. Peng, Y. Zhou, Y. Zhao, Y. Zhao, Z. Lu, M. Sun, C. Wu, H. Hu, H. Rao, T. Zhou and G. Su, *Chem. Eng. J.*, 2023, **466**, 143087.
47 Z. Jin, L. An and H. Zhang, *ACS Appl. Polym. Mater.*, 2023, **5**(4), 2704–2715.